JGE (Jurnal Geofisika Eksplorasi)
Vol. 08 No. 01, Maret 2022 (31-43) https://doi.org/10.23960/jge.v8i1.187

THE DIRECT-INVERSION DECONVOLUTION AND ITS APPLICATION IN SEISMIC DATA

DEKONVOLUSI DIRECT-INVERSION DAN APLIKASINYA PADA DATA SEISMIK

Iktri Madrinovella[1*], Waskito Pranowo[2]

[1,2]Geophysical Engineering, Pertamina University

Received: 2022, Januray 3rd
Accepted: 2022, February 11th

Keywords:
Deconvolution;
Direct-inversion;
Frequency;
Seismic enhancement.

Corespondent Email:
iktri.madrinovella@universitaspertamina.ac.id

How to cite this article:

Madrinovella, I. & Pranowo, W. (2022). The Direct-Inversion Deconvolution and Its Application in Seismic Data. *Jurnal Geofisika Eksplorasi*, 08(01), 31-43.

Abstract. Seismic traces are generated by the convolution of reflectivity and seismic wavelet. Due to limited frequency bandwidth, reflectivity can not be resolved easily. Deconvolution is a method to increase the frequency bandwidth and gives seismic data higher resolution, which makes it easier to analyze. Deconvolution is a common method in the seismic data processing. The mathematical definition of deconvolution is an inverse process of convolution, but the computation of deconvolution uses convolution in its process (Wiener deconvolution). We explained a method that is direct from the mathematical definition. We refer to it as direct-inversion deconvolution. The direct-inversion deconvolution process involves the matrix operation between seismic trace and wavelet instead of the deconvolution filter. By applying the direct-inversion deconvolution, the produced (or deconvolved) seismic trace shows a better result with higher resolution, regardless of the wavelet's phase. Finally, we performed a phase rotation experiment, and the deconvolution result shows no seismic phase alteration. In comparison, we also perform spiking deconvolution in synthetic data experiments. This method is applied to The North Sea Volve Data Village seismic data, and more thin layers are significantly detected. Finally, it turns out that direct-inversion deconvolution gives a higher resolution to seismic data.

Abstrak. *Trace seismik diperoleh dari konvolusi antara reflektivitas dan wavelet seismik. Karena adanya keterbatasan bandwidth frekuensi, reflektivitas tidak dapat teresolusi dengan baik. Dekonvolusi merupakan suatu metode untuk meningkatkan bandwidth frekuensi dan memberikan data seismik resolusi yang lebih tinggi, sehingga data seismik lebih mudah untuk dianalisis. Dekonvolusi merupakan metode umum dalam pengolahan data seismik. Definisi matematis dari dekonvolusi adalah proses pembalikan dari konvolusi, tetapi perhitungan proses dekonvolusi menggunakan konvolusi (dekonvolusi Wiener). Kami menjelaskan sebuah metode untuk memberikan makna langsung dari definisi matematisnya, yang kami sebut dengan direct-inversion dekonvolution. Proses direct-inversion dekonvolution melibatkan operasi matriks antara trace seismik dengan wavelet,*

bukan menggunakan filter dekonvolusi. Dengan menerapkan dekonvolusi real, trace seismik yang dihasilkan (atau didekonvolusikan) menunjukkan hasil yang lebih baik dengan resolusi yang lebih tinggi, terlepas dari fasa wavelet-nya. Kami melakukan percobaan rotasi fase, dan hasil dekonvolusi tidak menunjukkan perubahan fase seismik. Sebagai perbandingan, kami juga melakukan dekonvolusi Spiking dalam eksperimen data sintetis. Metode ini diterapkan pada data seismik The North Sea Volve Data Village. Hasilnya, terdapat lapisan tipis terdeteks. Jadi, dekonvolusi inversi langsung memberikan resolusi yang lebih tinggi untuk data seismik.

1. INTRODUCTION

Deconvolution is a method for the enhancement of seismic's vertical resolution, an essential part of seismic data processing and interpretation. Deconvolution's purpose is to broaden the frequency bandwidth by compressing the seismic wavelet. The seismic frequency is expected to provide broader bandwidth to obtain a higher resolution of seismic data and more thin layers to be resolved. These methods are commonly applied in oil industries to represent subsurface reflectivity better.

There are different types of known deconvolution: spiking deconvolution and predictive deconvolution (Yilmaz, 2001) based on Wiener filtering (Wiener, 1949), assuming the wavelet is stationary or does not change with travel time. However, the seismic wavelet varies in time and depth due to frequency attenuation and wavefront divergence (nonstationary). Therefore, the deconvolution theory proposed some alternatives to solve the nonstationary case.

First, inverse Q-filtering compensates for the frequency attenuation described by quality factor Q (van der Baan, 2012; Wang, 2006). However, this method requires pretty accurate Q-values, which is difficult to obtain in practice. The Q-value affects both seismic frequency and amplitudes. On the other hand, the seismic amplitude is also affected by reflectivity. Then, this may cause uncertainty in Q estimation. Moreover, the Q-value may be different each time (time-varying). There is research that tried to solve the problems (Merouane & Yilmaz, 2017). However, it has not been tested in real data.

Second, Gabor deconvolution combines the essential ideas of stationary deconvolution and inverse Q filtering (Margrave et al., 2011), or assuming seismic traces are split into segments which are called the molecular-Gabor transform (Wang et al., 2013). Finally, in recent developments, time-varying deconvolution uses the less-assumption technique in its processes, such as using S-transform (Jia et al., 2017; Winardhi & Pranowo, 2019) or other mathematical approaches (Pranowo, 2019; van der Baan, 2008).

A method also uses the modified S-transform (Djeffal et al., 2016), and another method to increase vertical resolution using improved time-frequency spectral modeling, provided by the decomposition of seismic trace using a generalized S-transform (Zhou et al., 2016). Mathematically, deconvolution is defined as the inverse convolution process by focusing on the basic theory of deconvolution. However, in practice, most deconvolution methods are computed using convolution.

This paper explained the direct-inversion deconvolution, which gives direct meaning to the mathematical definition. Furthermore, the example of applications in synthetic and real data are also performed. The result of this method is compared to spiking or Wiener deconvolution.

2. LITERATURE REVIEW

Seismic interpretation and reservoir characterization mostly relies on using relatively narrow bandwidth seismic datasets. To enable the full picture to be seen and characterized, the full frequency spectrum is needed (Reiser et al., 2012). At least, the frequency spectrum is broadened,

which can be achieved by using the deconvolution method.

In seismic data analysis theory, the subsurface reflectivity can be derived by deconvolving the wavelet with seismic traces (Goupillaud, 1961; Wuenschel, 1960). The deconvolution defines the deconvolved seismic trace as the reflectivity by inverting the process of convolution instead of using a Wiener filter (Wiener, 1949). The result shows the deconvolved seismic trace as the reflectivity. In this paper, we refer to this deconvolution as direct-inversion deconvolution.

The direct-inversion deconvolution method has a different procedure. The deconvolved seismic trace is not generated by using the Wiener filter. Practically, the procedure only needs the seismic trace and the inverse matrix of the wavelet. In addition, pre-whitening is still needed to handle an ill-conditioned matrix.

Direct-inversion deconvolution is not common. This process is rarely used in deconvolution, even though it exists. This is because of the causation of the matrix's singularity and ill-condition. However, this paper shows that this method can be applied in a synthetic seismogram (which is generated by synthetic reflectivity and certain wavelet) and a real data seismic. It can also increase the data resolution.

2.1. Seismic Trace, Convolution, and Deconvolution

Synthetic seismogram or trace is given by convolution model between wavelet and reflectivity series (Goupillaud, 1961; Wuenschel, 1960). This model is expressed by,

$$s(t) = r(t) * w(t) \quad (1)$$

where $s(t)$ is synthetic seismogram, $r(t)$ is reflectivity series, $w(t)$ is wavelet, and $*$ is a convolution operation. The process of Eq.1 is illustrated by **Figure 1**. Wavelet represents seismic pulse or signal of seismic energy source, while reflectivity series represents the contrast of acoustic impedance between the layer of rocks and signs of layer boundaries.

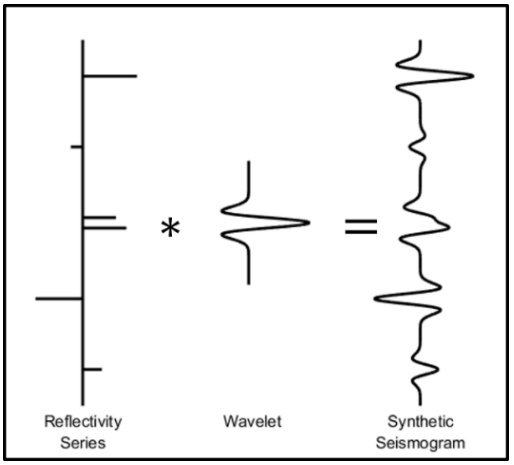

Figure 1. Synthetic seismogram modeling based on Eq. 1.

Deconvolution is the inverse process of the convolution model. Because the convolution gives seismic trace, the deconvolution produces reflectivity series. In both deconvolution and convolution, the wavelet is assumed as a known variable or at least can be estimated.

2.2. Wiener and Spiking Deconvolution

Wiener deconvolution is intended to modify an input signal to be the desired output using the convolution process (Wiener, 1949; Yilmaz, 2001). Let a seismic trace be input and reflectivity be the desired output, then

$$R(t) = F(t) * S(t) \quad (2)$$

where $S(t)$ is a seismic trace, $F(t)$ is Wiener filter, $R(t)$ is a reflectivity series, and $*$ is a convolution operation. Eq.2 can be written in matrix operation as

$$\mathbf{R} = \mathbf{FS} \quad (3)$$

where **S** is a vector of seismic trace, **F** is a matrix of moving Wiener filter, and **R** is a vector of reflectivity.

The Wiener filter is designed so the input can be the desired output. The relationship between input, desired output, and Wiener filter can be expressed as matrix operation as,

$$\underbrace{\begin{bmatrix} c_0 \\ c_1 \\ \vdots \\ c_n \end{bmatrix}}_{\mathbf{C}} = \underbrace{\begin{bmatrix} a_0 & a_{-1} & \cdots & a_{-n} \\ a_1 & a_0 & \cdots & a_{-(n-1)} \\ \vdots & \vdots & \ddots & \vdots \\ a_n & a_{n-1} & \cdots & a_0 \end{bmatrix}}_{\mathbf{A}} \underbrace{\begin{bmatrix} f_0 \\ f_1 \\ \vdots \\ f_n \end{bmatrix}}_{\mathbf{F}} \quad (4)$$

where **F** is Wiener filter, **A** is Toeplitz matrix of input autocorrelation and **C** is cross-correlation between input and desired output. Indeed, the Wiener filter can be obtained by,

$$\mathbf{F} = (\mathbf{A} + \lambda\mathbf{I})^{-1}\mathbf{C} \quad (5)$$

where λ is pre-whitening. If our desired output is a spike, **C** can be replaced with,

$$\mathbf{C} = [1,0,\dots,0]^{\mathrm{T}} \quad (6)$$

Then, the process is known as spiking deconvolution (Yilmaz, 2001). The filter **F** is convolved with a seismic trace to get the reflectivity, as shown in Eq.2. In reality, the result of Wiener (or spiking) deconvolution can be reflectivity. It is a broadened frequency (or enhanced) seismic trace. So, Eq.2 can be written as,

$$\mathbf{S}_{decon} = \mathbf{FS} \quad (7)$$

By mathematical definition, deconvolution is the inverse process of convolution. On the other hand, Wiener deconvolution (and its derivatives) uses convolution in its process, which sounds contradictory to its definition. However, because of its result, the Wiener deconvolution is still classified as a seismic deconvolution method. Any method can be considered a seismic deconvolution as long as it can or is intended to produce a reconstructed reflectivity from a seismic trace.

2.3. Direct-inversion Deconvolution

The convolution process in Eq.1 can be written as matrix operation as,

$$\mathbf{S} = \mathbf{WR} \quad (8)$$

where **S** is seismic trace, **R** is reflectivity, and **W** is a matrix of moving or shifting wavelet (**Figure 2**).

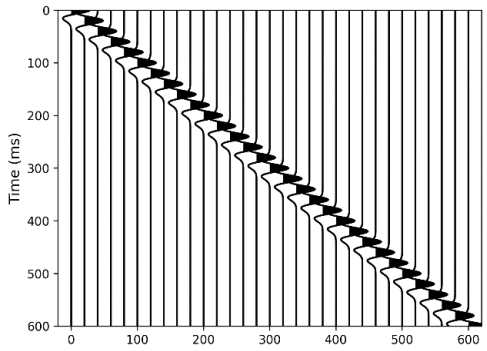

Figure 2. Matrix of moving wavelet.

From Eq.7, **R** is obtained with the objective function by minimizing L_2 norm of,

$$\min_{\mathbf{R}} \|\mathbf{S} - \mathbf{WR}\|_2 \quad (9)$$

where $\|\cdot\|_2$ is L_2 norm. The objective function is achieved by using matrix inversion (Meresescu, 2019),

$$\mathbf{R} = \mathbf{W}^{-1}\mathbf{S} \quad (10)$$

However, **W** is usually an ill-conditioned matrix (**Figure 3**). One way to overcome this problem is to add the pre-whitening (or damping) in the inversion process, so

$$\mathbf{R} = (\mathbf{W} + \lambda\mathbf{I})^{-1}\mathbf{S} \quad (11)$$

where λ is a pre-whitening.

The pre-whitening handles not only the ill-conditioned matrix but also noise presence. A lower signal-to-noise ratio requires a higher λ. However, Eq.10 sometimes does not handle noise well. Therefore, Eq.8 can be solved using pseudo-inverse,

$$\mathbf{R} = \left(\mathbf{W}^{\mathbf{T}}\mathbf{W} + \lambda\mathbf{I}\right)^{-1}\mathbf{W}^{\mathbf{T}}\mathbf{S} \quad (12)$$

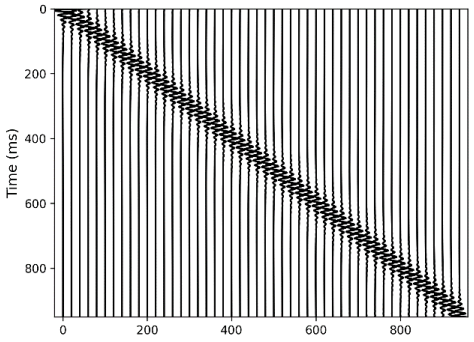

Figure 3. $(\mathbf{W}^{\mathbf{T}}\mathbf{W} + \lambda\mathbf{I})^{-1}\mathbf{W}^{\mathbf{T}}$.

Eq.12 performs the inverse process of deconvolution. So, it can be considered as direct-inversion deconvolution. However, it is hard to produce reflectivity from a seismic trace in reality. It is because the seismic frequency is band-limited. Instead of producing reflectivity, Eq.12 produces a deconvolved (or enhanced) seismic trace. So, it is wiser to change **R** in Eq.12 similar to Eq.7 as,

$$\mathbf{S_{decon}} = \left(\mathbf{W^T W} + \lambda \mathbf{I}\right)^{-1} \mathbf{W^T S} \qquad (13)$$

where $\mathbf{S_{decon}}$ is a deconvolved seismic trace.

If the wavelet's phase is unknown or uncertain, the wavelet in **W** is set zero-phase. If we set **W** is set zero-phase, it does not alter the original seismic phase. However, it is permissible to add wavelet phase in **W**. There are several methods in phase estimation (Fomel & van der Baan, 2014). If we add phase in **W**, the direct-inversion deconvolution will de-phasing $\mathbf{S_{decon}}$. In fact, the deconvolution process in Eq. 12 is used implicitly in seismic inversion. For example, model-based inversion uses Eq.12 in its equation (Hampson-Russel Software, 1999; Pranowo, 2019).

3. METHODS

3.1. Data

This paper uses three datasets: 2 synthetic and real datasets. The synthetic datasets contain 2 cases. The first is synthetic data with very sparse reflectivity (**Figure 4**). The other one is synthetic data with denser reflectivity (**Figure 5**). Each synthetic seismic trace is generated by convolving synthetic reflectivity with Ricker Wavelet 25 Hz. The synthetic data is used to know the behavior of the direct-inversion deconvolution. Meanwhile, the application in real data (**Figure 6**) is to see whether the direct-inversion deconvolution is applicable in real conditions. The real data is Equinor's Open Data: The North Sea Volve Data Village (Equinor, 2018).

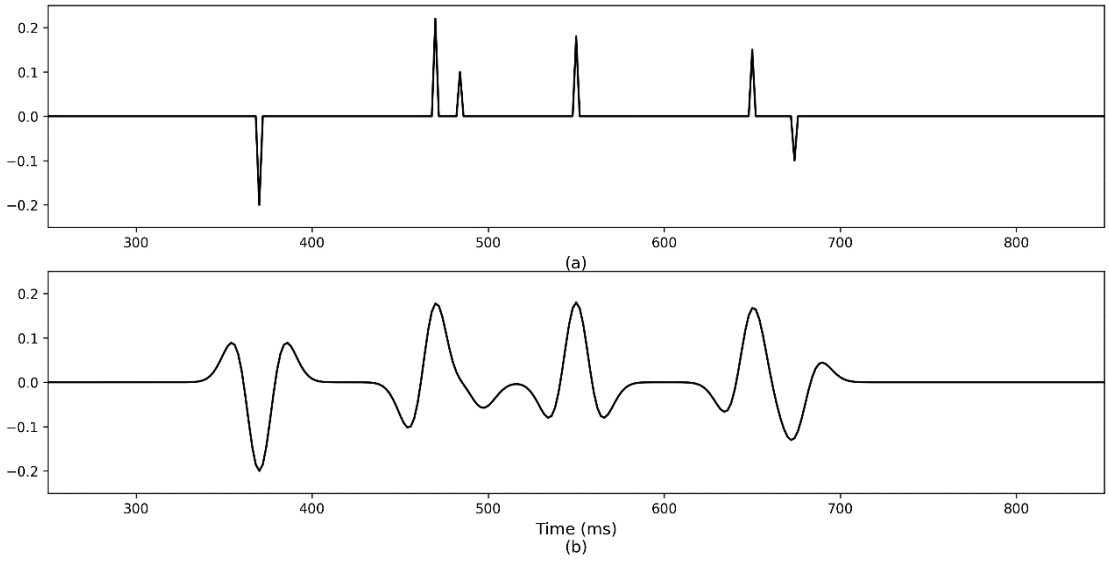

Figure 4. Sparser Cases Synthetic Data: Reflectivity (a) and Seismic Trace (b).

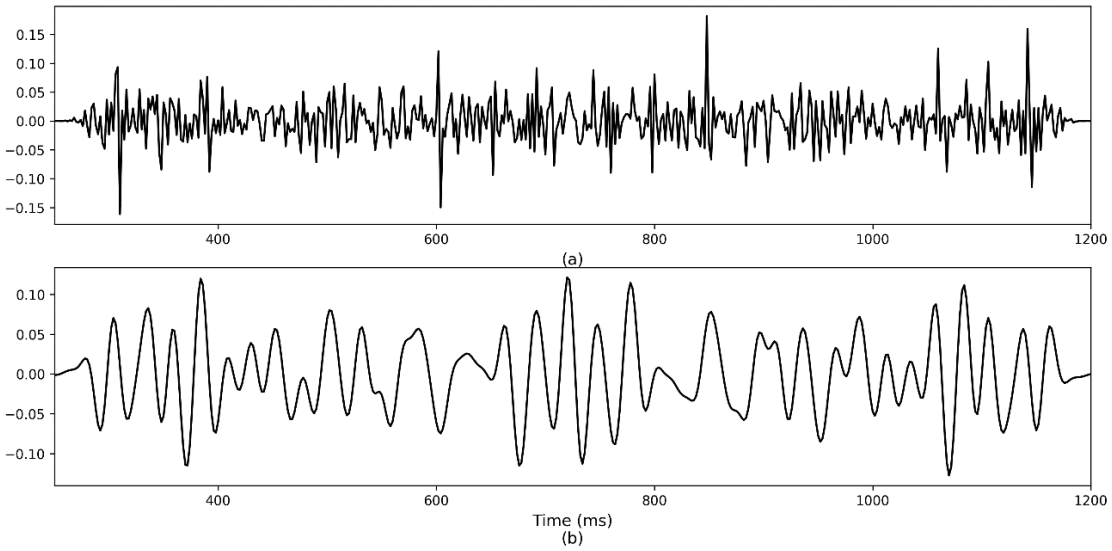

Figure 5. Denser Cases Synthetic Data: Reflectivity (a) and Seismic Trace (b).

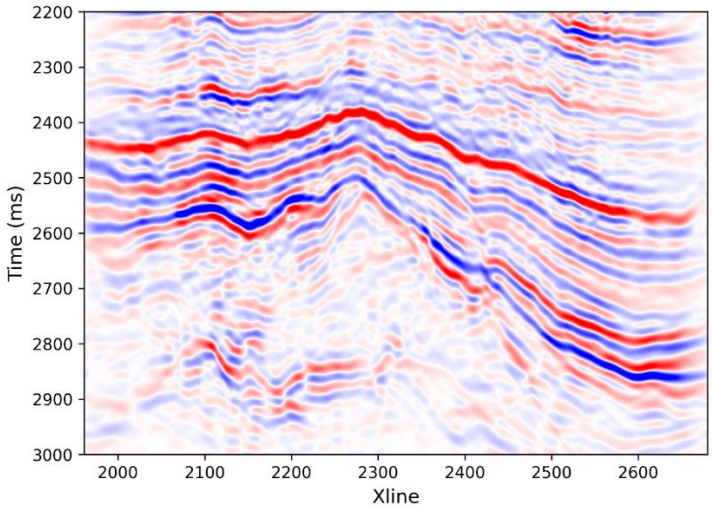

Figure 6. The North Sea Volve Village Seismic Data.

3.2. Methods

This paper uses direct-inversion deconvolution as the main method. The procedure of direct-inversion deconvolution in a real application:

a. Extract the wavelet from the seismic data. We suggest using a statistical wavelet (Cui & Margrave, 2014).
b. Construct moving wavelet matrix (**Figure 2**).
c. Determine pre-whitening in Eq. 12. We suggest the pre-whitening between 1% to 10%, depending on S/N.
d. Apply direct-inversion deconvolution (Eq. 12).

4. RESULTS AND DISCUSSION

4.1. Application to Synthetic Data

Figure 7 shows the result of the direct-inversion deconvolution method to a synthetic seismic trace for the sparser case. The deconvolved seismic trace (**Figure 7b**) gives a better resolution than the original (**Figure 7a**). The interfered reflectors more separated after deconvolution. The result is consistent with the denser case (**Figure 8**).

Many reflectors appear, and the wavelet is seen to become narrowed. In the sparser case, there are ringing phenomena from wavelet sidelobes. This is called Gibb's phenomenon, not caused by inversion instability or noise. The direct-inversion deconvolution attempts to broaden bandwidth as much as possible. The consequence of broadening the spectrum to a higher frequency is that the wavelet becomes sharper than the original, but the ringing amplitude appears. Meanwhile, broadening the spectrum to a lower frequency makes wavelet sidelobes' amplitudes become small.

Increasing the amplitude of the spectrum towards higher frequencies will always result in ringing. This is a trade-off of increasing the frequency. The application of a taper only reduces the effect, but the ringing is still there. **Figure 11** and **12** illustrate how a wider bandwidth can cause ringing. In **Figure 11a**, there is an amplitude spectrum jump at 125 Hz. This causes a ringing from -∞ to ∞ in the time domain (**Figure 12a**). In **Figure 11b**, a taper is applied to the spectrum of **Figure 11a**. In the time domain, the wavelet of image **Figure 12b** still shows ringing, although it is less than **Figure 12a**. If we widen the taper (**Figure 12c**), the ringing is much reduced. However, **Figure 12c** shows a bandwidth that is not as wide as **Figure 12b**. **Figure 11d** is a spectrum belonging to the wavelet ricker wherein the time domain; there is only 1 pair of sidelobes without ringing (**Figure 12d**). Therefore, ringing presence is unavoidable due to frequency widening, even though a taper is applied.

To test the ability of deconvolution to face nonzero-phase seismic data, we rotate the synthetic data's phase 45° (**Figure 9a** and **10a**). Then, we perform the same deconvolution parameter like in **Figure 7** and **8**. It should be emphasized that, although we shift the seismic data phase to 45°, we do not shift the wavelet in matrix **W** (Eq. 10). This is performed to simulate the real application, that wavelet seismic phase is difficult to predict.

The results of deconvolution are shown in **Figure 9b** and **10b**. The seismic trace is seen to have a higher resolution. Interest-ingly, the direct-inversion deconvolution does not alter the seismic phase. After deconvolution, the seismic phases are still 45°. Then, directinversion deconvolution is applied for any seismic phase.

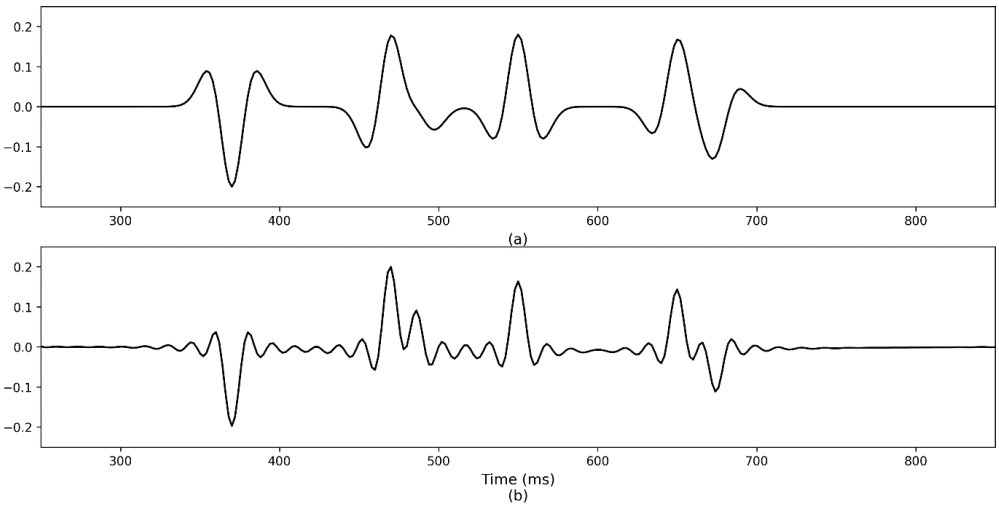

Figure 7. Original (a) and deconvolved seismic trace (b) for the sparser case.

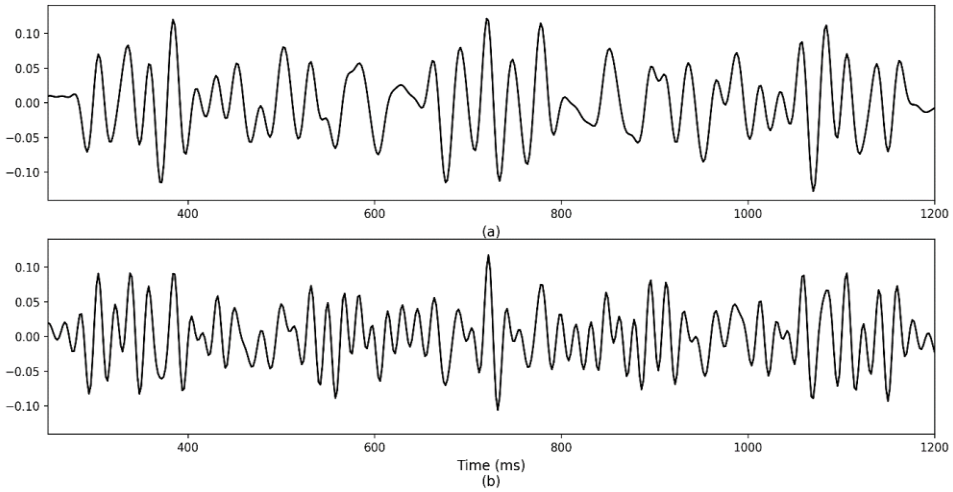

Figure 8. Original (a) and deconvolved seismic trace (b) for the denser case.

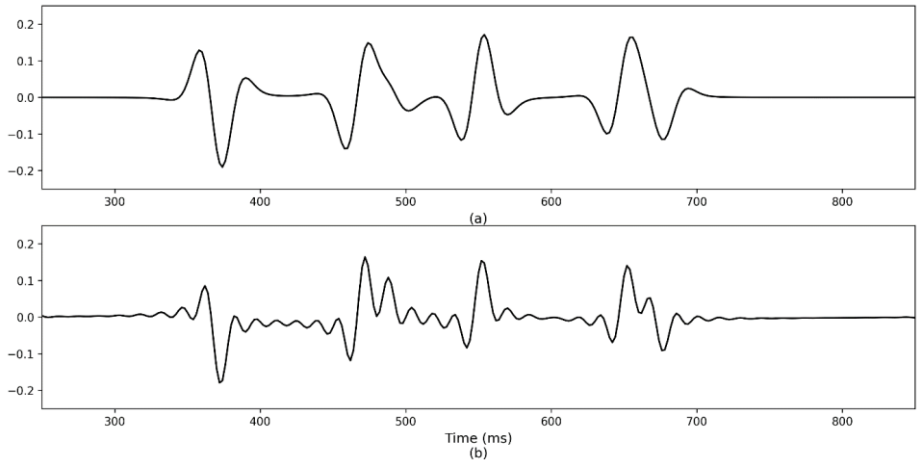

Figure 9. Original (a) and deconvolved seismic trace (b) with phase rotation 45° for the sparser case.

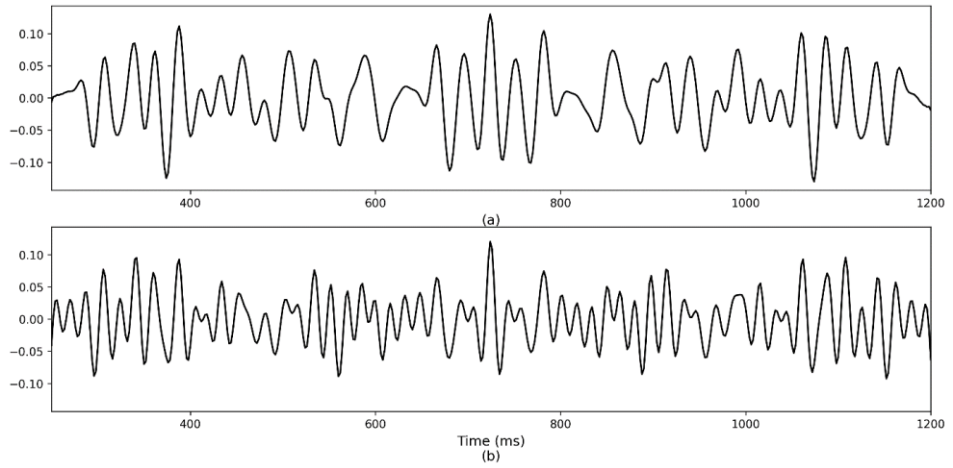

Figure 10. Original (a) and deconvolved seismic trace (b) with phase rotation 45° for the denser case.

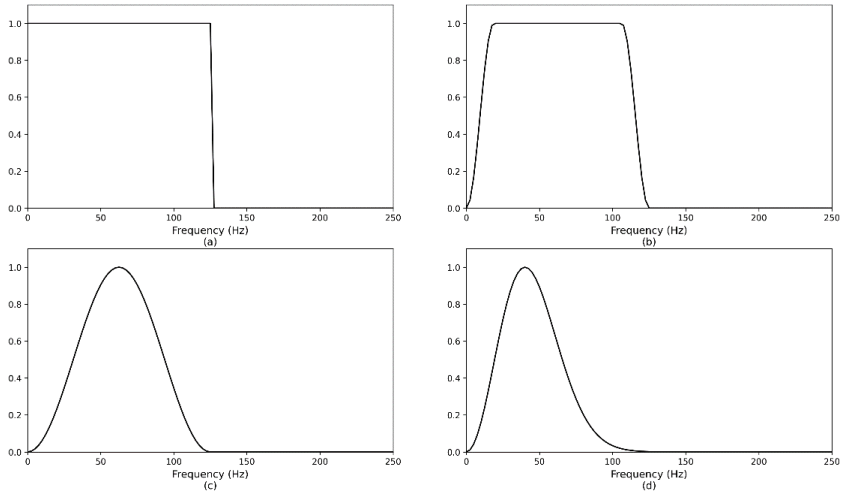

Figure 11. Wavelets' amplitude spectrums: (a) boxcar-shaped spectrum, (b) Tukey-shaped (tapered boxcar) spectrum, (c) Hann-shaped spectrum, and (d) Ricker wavelet's spectrum.

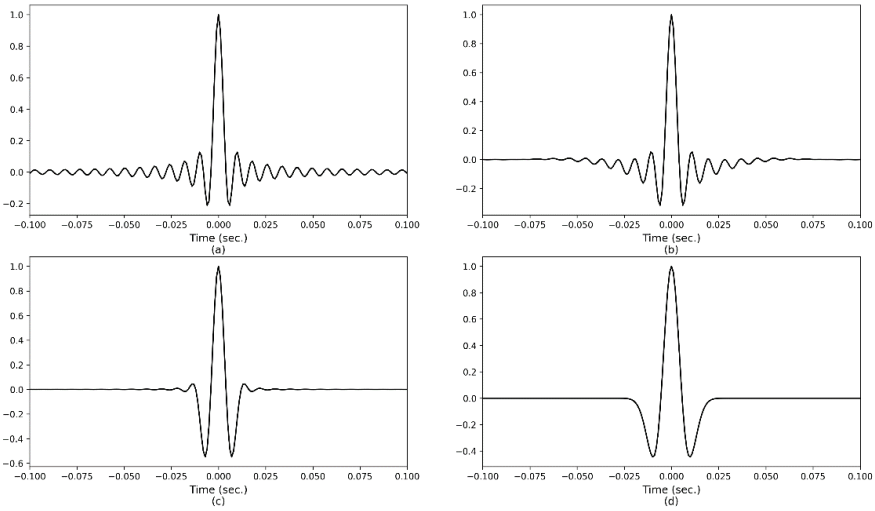

Figure 12. The wavelets (in the time domain) correspond to amplitude spectrums in Figure 11.

We also compare the direct-inversion deconvolution with Wiener deconvolution to know the difference. **Figure 11** shows the comparison between direct-inversion deconvolution (**Figure 11b**) and spiking deconvolution (**Figure 11c**). This figure shows that spiking deconvolution produces a trace with a higher resolution.

However, as can be seen, the seismic phase changes. This is because Spiking (and Wiener) deconvolution uses the assumption of minimum phase (Cary, 2001; Yilmaz, 2001). Unlike spiking, direct-inversion deconvolution does not alter the seismic phase while enhancing the resolution. We add band-limited noise to the sparse case synthetic trace to know how direct-inversion deconvolution behaves in noise presence (**Figure 12a**). **Figure 12b** shows that direct-inversion deconvolution does not boost the noise amplitudes.

4.2. Application to Real Data

The original seismic data has a limited bandwidth of frequency which does not resolve the thinner layers. **Figure 13** illustrates the enhanced resolution after the application of the direct-inversion deconvolution. **Figure 13a** is the field data,

and **Figure 7b** shows the result after the direct-inversion deconvolution is performed. Thinner layers are detected at shallow depth (2200–2600 ms). This concludes that the direct-inversion deconvolution method improves the resolution so that the seismic data can be interpreted and analyzed more easily. In the deconvolution process, we have to estimate the wavelet. This paper uses a statistical wavelet.

We can see the seismic's spectrums to know how broad seismic bandwidth is enhanced (**Figure 14**). The deconvolved seismic's spectrum (red area) has broader bandwidth than the original data (black area). The direct-inversion deconvolution, like other methods, cannot enhance bandwidth to broad. It only can broaden the bandwidth to the frequency the original data can retain

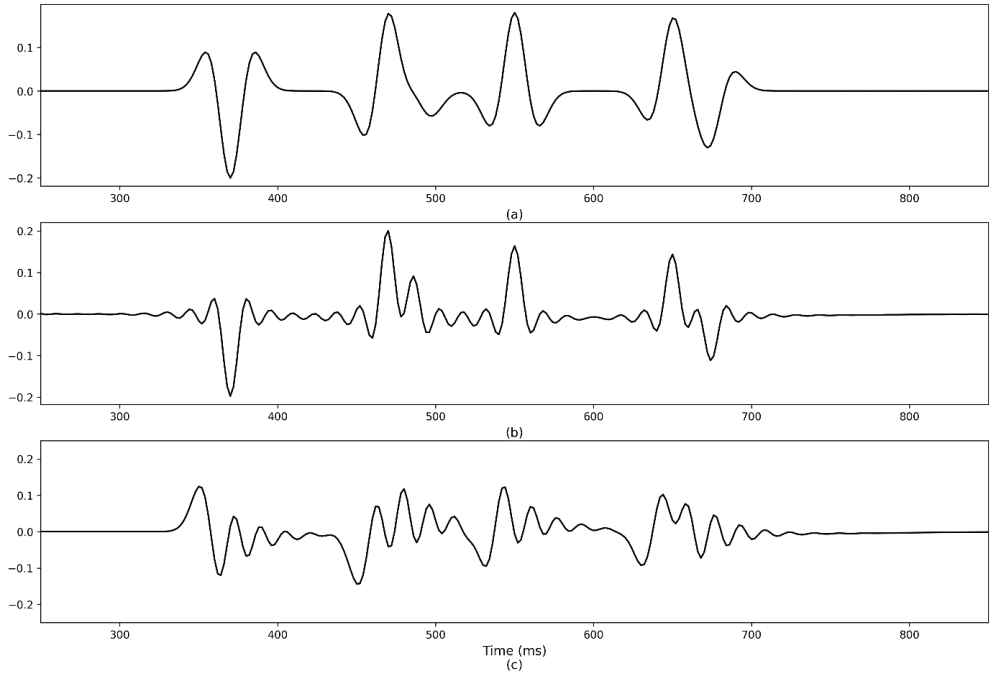

Figure 13. Comparison between original (a), real deconvolved (b), and spiking deconvolved-(c) trace.

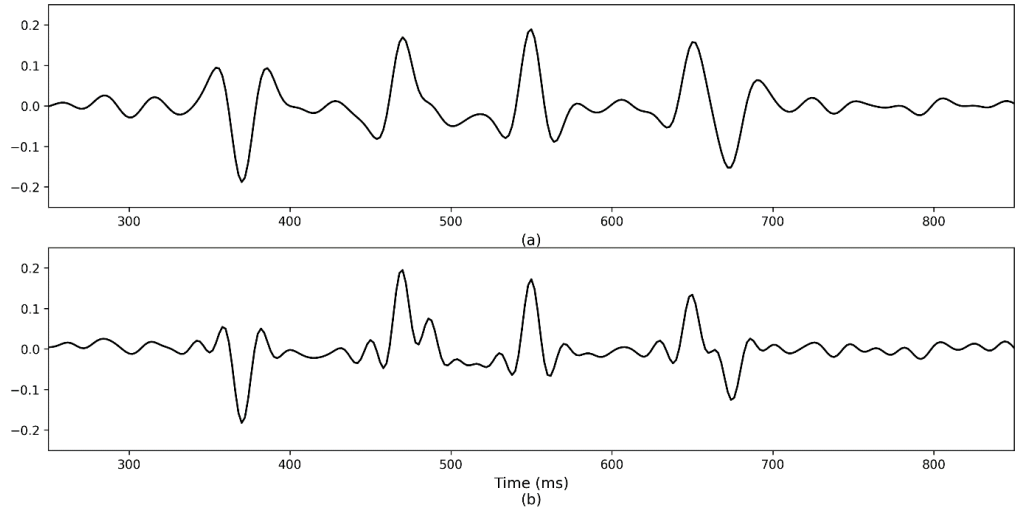

Figure 14. Original (a) and deconvolved seismic trace (b) with band-limited noise.

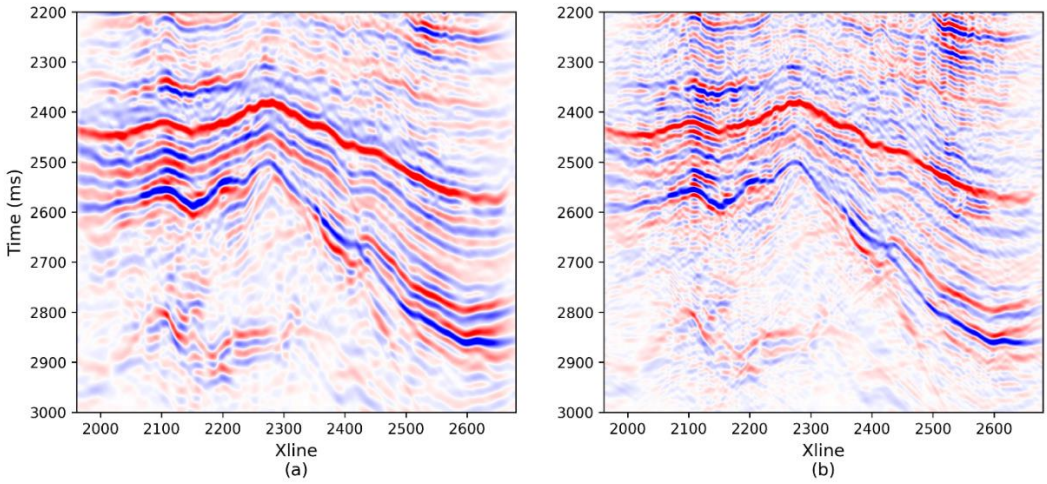

Figure 15. Real data application. Before (a) and after (b) deconvolution.

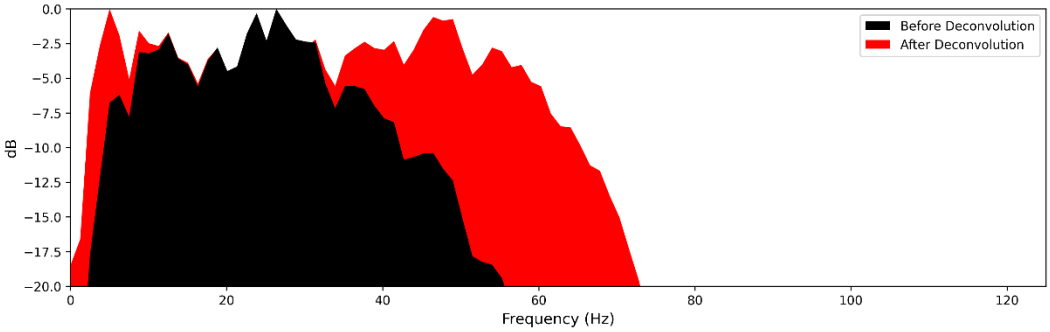

Figure 16. The spectrums of real data before (black) and after (red) deconvolution.

The point of this method is the inverse process of deconvolution as theory defined, without using the Wiener filter known as spiking or Wiener deconvolution (Yilmaz, 2001; Wiener, 1949). In **Figure 9** and **10**, the direct-inversion deconvolution result shows that this method is not dependent on the wavelet phase. It is unnecessary to assume that the phase is a minimum phase or to rotate the original phase to the minimum phase.

Apart from its advantages, the direct-inversion deconvolution has several cautious. Firstly, we have to predict the wavelet shape, not its phase. The error of wavelet estimation may affect the deconvolution result. The second is Gibb's phenomenon appearance. Actually, this phenomenon is expected since we boost to the higher frequency. The filter-based deconvolution uses the taper function to reduce this phenomenon, not to get rid. However, it cannot be applied to direct-inversion deconvolution unless we apply an additional step.

This method can be applied in the stationary case. However, it should be developed or combined with other methods to solve the nonstationary problems.

5. CONCLUSION

The direct-inversion deconvolution process is performed according to the mathematical definition of deconvolution. The results are shown by deconvolved seismic trace instead of reflectivity and the better version of the seismic image. This method is applied to synthetic data using synthetic reflectivity and Ricker Wavelet 25 Hz, and it gives a higher resolution to the seismic data. A phase rotation does not affect the deconvolution result, which means the result is not influenced by or dependent on the wavelet's phase. The real data also shows

a higher resolution after the direct-inversion deconvolution is applied. More thin layers can be seen more clearly, and the frequency bandwidth is broadened to the frequency the original data can retain.

ACKNOWLEDGMENT

We thank Dr. Arif Ismul Hadi, M.Si. and anonymous reviewer for the suggestions for the manuscript. We also thank Equinor for the open seismic data (The North Sea Volve Data Village).

REFERENCES

Cary, P. W. (2001). Seismic Deconvolution: Assumptions, Concerns and Convictions. *CSEG Recorder*, 27–28. https://csegrecorder.com/articles/view/seismic-deconvolution-assumptions-concerns-and-convictions

Cui, T., & Margrave, G. F. (2014). Seismic wavelet estimation. *CREWES Research Report*, *26*, 1–16. https://www.crewes.org/ForOurSponsors/ResearchReports/2014/CRR201418.pdf

Djeffal, A., Pennington, W., & Askari, R. (2016). Enhancement of Margrave deconvolution of seismic signals in highly attenuating media using the modified S-transform. *SEG Technical Program Expanded Abstracts 2016*, *1*, 5198–5202. https://doi.org/10.1190/segam2016-13971963.1

Equinor. (2018). *Equinor's Open Data: The North Sea Volve Data Village*. https:data.equinor.com

Fomel, S., & van der Baan, M. (2014). Local skewness attribute as a seismic phase detector. *Interpretation*, *2*(1), SA49–SA56. https://doi.org/10.1190/INT-2013-0080.1

Goupillaud, P. L. (1961). An Approach to Inverse Filtering of Near-surface Layer Effects from Seismic Records. *GEOPHYSICS*, *26*(6), 754–760. https://doi.org/10.1190/1.1438951

Hampson-Russel Software. (1999). *STRATA Theory* (p. 13). Hampson-Russell Software Services Ltd. https://www.cgg.com/data/1/rec_docs/585_STRATA_Theory.pdf

Jia, J., Chen, X., Jiang, S., Jiang, W., & Zhang, J. (2017). Resolution enhancement in the generalized S-transform domain based on variational-mode decomposition of seismic data. *International Geophysical Conference, Qingdao, China, 17-20 April 2017*, *April*, 315–318. https://doi.org/10.1190/IGC2017-082

Margrave, G. F., Lamoureux, M. P., & Henley, D. C. (2011). Gabor deconvolution: Estimating reflectivity by nonstationary deconvolution of seismic data. *GEOPHYSICS*, *76*(3), W15–W30. https://doi.org/10.1190/1.3560167

Meresescu, A.-G. (2019). *Inverse Problems of Deconvolution Applied in the Fields of Geoscience and Planetology*. Université Paris Saclay.

Merouane, A., & Yilmaz, O. (2017). Time-varying Q estimation on reflection seismic data in the presence of amplitude variations. *SEG Technical Program Expanded Abstracts 2017*, 3552–3556. https://doi.org/10.1190/segam2017-17782597.1

Pranowo, W. (2019). Time-varying wavelet estimation and its applications in deconvolution and seismic inversion. *Journal of Petroleum Exploration and Production Technology*, *9*(4), 2583–2590. https://doi.org/10.1007/s13202-019-00748-9

Reiser, C., Bird, T., Engelmark, F., Anderson, E., & Balabekov, Y. (2012). Value of broadband seismic for interpretation, reservoir characterization and quantitative interpretation workflows. *First Break*, *30*(9). https://doi.org/10.3997/1365-2397.30.9.62319

van der Baan, M. (2008). Time-varying wavelet estimation and deconvolution by kurtosis maximization. *GEOPHYSICS*, *73*(2), V11–V18. https://doi.org/10.1190/1.2831936

van der Baan, M. (2012). Bandwidth enhancement: Inverse Q filtering or time-varying Wiener deconvolution? *GEOPHYSICS*, *77*(4), V133–V142. https://doi.org/10.1190/geo2011-0500.1

Wang, L., Gao, J., Zhao, W., & Jiang, X. (2013). Enhancing resolution of nonstationary seismic data by molecular-Gabor transform. *GEOPHYSICS*, *78*(1), V31–V41. https://doi.org/10.1190/geo2011-0450.1

Wang, Y. (2006). Inverse Q -filter for seismic resolution enhancement. *GEOPHYSICS*, *71*(3), V51–V60. https://doi.org/10.1190/1.2192912

Wiener, N. (1949). Minimization of RMS Error. In *The Interpolation, Extrapolation and Smoothing of Stationary Time Series* (pp. 131–133).

Winardhi, S., & Pranowo, W. (2019). Multi-Ricker Spectral Modeling in the S-transform Domain for Enhancing Vertical Resolution of Seismic Reflection Data. *Indonesian Journal on Geoscience*, *6*(3).

https://doi.org/10.17014/ijog.6.3.223-233

Wuenschel, P. C. (1960). Seismogram Synthesis Including Multiples and Transmission Coefficients. *GEOPHYSICS*, *25*(1), 106–129. https://doi.org/10.1190/1.1438677

Yilmaz, Ö. (2001). *Seismic Data Analysis*. Society of Exploration Geophysicists. https://doi.org/10.1190/1.9781560801580

Zhou, H., Wang, C., Marfurt, K. J., Jiang, Y., & Bi, J. (2016). Enhancing the resolution of non-stationary seismic data using improved time–frequency spectral modelling. *Geophysical Journal International*, *205*(1), 203–219. https://doi.org/10.1093/gji/ggv553